

Self-healing cementitious composites with a hollow vascular network created using 3D-printed sacrificial templates

Wan, Zhi; Zhang, Yu; Xu, Yading; Šavija, Branko

DOI

[10.1016/j.engstruct.2023.116282](https://doi.org/10.1016/j.engstruct.2023.116282)

Publication date

2023

Document Version

Final published version

Published in

Engineering Structures

Citation (APA)

Wan, Z., Zhang, Y., Xu, Y., & Šavija, B. (2023). Self-healing cementitious composites with a hollow vascular network created using 3D-printed sacrificial templates. *Engineering Structures*, 289, Article 116282. <https://doi.org/10.1016/j.engstruct.2023.116282>

Important note

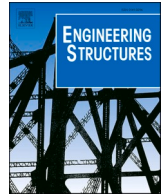
To cite this publication, please use the final published version (if applicable). Please check the document version above.

Copyright

Other than for strictly personal use, it is not permitted to download, forward or distribute the text or part of it, without the consent of the author(s) and/or copyright holder(s), unless the work is under an open content license such as Creative Commons.

Takedown policy

Please contact us and provide details if you believe this document breaches copyrights. We will remove access to the work immediately and investigate your claim.



Self-healing cementitious composites with a hollow vascular network created using 3D-printed sacrificial templates

Zhi Wan^{*}, Yu Zhang, Yading Xu, Branko Šavija

Microlab, Faculty of Civil Engineering and Geosciences, Delft University of Technology, Delft, The Netherlands

ARTICLE INFO

Keywords:

3D printing
Self-healing concrete
Polyvinyl alcohol
Vascular network
Healing efficiency

ABSTRACT

Additively manufactured vascular networks have great potential for use in autonomous self-healing of cementitious composites as they potentially allow multiple healing events to take place. However, the existence of a vascular tube wall may impede with the healing efficiency if it does not rupture timely to release the healing agent. The issue of vascular material design has therefore been a major topic of research. To overcome this, dissolvable Polyvinyl Alcohol (PVA) filament is adopted in this study to fabricate the vascular networks. Fabricated networks are coated with wax, placed in cementitious mortar and removed upon hardening, thereby leaving a network of hollow channels. Different printing directions were expected to affect the dissolvability of printed structures and were therefore fabricated and tested. Different shapes (i.e., 2D and 3D) of vascular networks were printed and embedded in the cementitious mortar. Four-point bending tests and permeability tests were performed to investigate the healing efficiency. Multiple healing cycles were applied in the cracked specimens. The results show that the vertically printed PVA tubes with wax coating have good dissolution behaviour. As expected, the existence of vascular networks decreases the initial flexural strength of the specimens. In terms of healing efficiency, excellent mechanical and water tightness recovery were achieved when using epoxy resin as the healing agent. The mechanical recovery after the first healing process is higher than the following healing process. The watertightness of the cracked samples keeps decreasing with the increase of healing cycles. Specimens embedded with 3D vascular networks have higher healing potential than those utilizing 2D vascular networks.

1. Introduction

Degradation of concrete structures is inevitable due to concrete susceptibility to cracking, resulting in significant maintenance and repair costs [1,2]. Among the possible crack-repair strategies, self-healing concrete is promising as cracks are repaired with no or little human intervention [3]. Early studies in self-healing concrete focused on improving the autogenous healing process by using mineral additions [4,5], crystalline admixtures [6,7], superabsorbent polymers [8,9] to stimulate ongoing hydration or crystallization. However, autogenous healing is limited to small crack widths (less than 200 μm) [10]. Encapsulation of a healing agent is another effective method to heal the cracks [11,12,13]. Except for polymers or minerals, bacteria producing calcium carbonate could also be encapsulated to heal the cracks [14,15,16].

Inspired by human cardiovascular system and plant vascular tissue system, embedding vascular networks in a host matrix enables

transporting healing agents to the crack region [17]. The main advantage of the vascular based self-healing material is the continuous supply of healing agents, which facilitates healing of wider cracks and repeating the healing process [18,19]. Except for the healing agents [20], vascular material also plays a key role in the healing efficiency of vascular based self-healing cementitious composite. The vascular material must be strong enough to survive concrete mixing and casting, and brittle enough to fracture when cracks in concrete occur [21]. Borosilicate glass has been widely used as the encapsulation materials because of its brittleness [22,23,24]. However, glass is susceptible to alkali-silica reaction, which could affect the service life of the vascular network. Alternatively, brittle materials such as polymethyl methacrylate (PMMA), inorganic phosphate cement (IPC) [25] and polyvinyl chloride (PVC) [26] have been used to create the vascular networks. Recently, the development of additive manufacturing (AM) allowed fabricating vascular structures with complex geometry to improve the healing efficiency without significantly lowering the mechanical properties of

^{*} Corresponding author.

E-mail addresses: Z.Wan-1@tudelft.nl (Z. Wan), Y.Zhang-28@tudelft.nl (Y. Zhang), Y.Xu-5@tudelft.nl (Y. Xu), B.Savija@tudelft.nl (B. Šavija).

<https://doi.org/10.1016/j.engstruct.2023.116282>

concrete [19,20,27]. The selection of printing materials is still vital considering the bonding between the 3D-printed vascular network and cementitious matrix [28,29]. The existence of vascular tubes should be monitored in a long-term period to ensure its functionality for self-healing. In other words, such vascular networks still need to rupture timely to release the healing agent [30].

To overcome the problems caused by vascular tubes, hollow channels can be created inside the host matrix to serve as the path for transporting healing agents. In self-healing polymers or composites, sacrificial materials have been used to create the vascular network. After being embedded in the matrix, the vascular tubes are heated and then removed, leaving behind hollow channels. For example, a microvascular network has been used to promote self-healing process in polymers by fugitive ink (60 wt% petroleum jelly and 40 wt% microcrystalline wax) [31] or 300 μm sacrificial fibres [32]. Boba [33] used Nichrome wires coated with polylactic acid (PLA) between the composite layers. In the field of self-healing cementitious composites, sacrificial materials have not been used so far to fabricate hollow channels. Compared with self-healing polymers, the hollow channels in cementitious composites have so far been relatively simple. Early researchers preplaced solid bars in the moulds prior to concrete casting, which were subsequently removed after concrete setting to create hollow channels [34]. Inspired by the structure of bones, Sangadji and Schlangen [35] used porous network concrete as the flow path to heal the cracks. Similar to sacrificial materials, heat shrinking tubing or polyurethane tubing was used by Davies [36] to create a 2D vascular network in cementitious materials. However, these materials could only be used for creating relatively simple vascular networks. For creating three-dimensional vascular networks with additive manufacturing, Li et al. [30] investigated the feasibility of using Polyvinyl Alcohol (PVA) as the printing material. Based on the obtained result, they concluded that the main functional groups of extruded PVA remain unchanged with the un-extruded PVA, and that the highly alkaline environment of the cement paste does not affect the dissolution of the PVA. However, the volume expansion and reaction with cementitious matrix during the dissolution of PVA vascular networks have not yet been solved. Furthermore, a possible influence of the printing direction on the dissolution of PVA embedded in cementitious matrix has not been previously studied. More importantly, previous researches mainly design the vascular network towards higher mechanical properties using numerical simulation [37]. The experimental investigation on self-healing concrete with different shape of hollow channels as vascular network is rare.

Therefore, in this study, we carry out a comprehensive investigation of self-healing cementitious composite embedded with a sacrificial 3D-printed vascular network. The dissolution of 3D-printed PVA hollow tubes under different configurations, i.e., printing direction (horizontal/vertical), tube wall thickness/radius ratio, and coating condition (with/without wax coating) was studied first. After determining the fabricating configuration, PVA tubes and PLA connectors were printed, assembled and then embedded in the cementitious mortar. The influence of vascular shape (i.e., 2D and 3D) on the mechanical properties under 4-point bending is investigated. Subsequently, epoxy resin was injected as the healing agent to seal the cracks for multiple times. The healing efficiency in terms of mechanical property and water tightness recovery of the vascular based self-healing mortar is discussed.

2. Experiments

2.1. Fabrication and pre-processing of PVA vascular

One-dimensional hollow tubes were fabricated first to study the influence of fabrication configuration on the dissolution of PVA embedded in cementitious mortar. The designed tubes are sliced with Cura (Ultimaker, Utrecht, Netherlands) and then are printed with a commercial 3D printer Ultimaker 2+. The printing parameters are shown in Table 1.

According to the previous research [38], fused deposition modelling

Table 1
The used printing parameters.

Printing parameters	Value
Nozzle temperature (PVA, °C)	225
Nozzle temperature (PLA, °C)	210
Nozzle size (mm)	0.25
Bed plate temperature (°C)	60
Fan speed (%)	100
Printing speed (mm/s)	30
Layer height (mm)	0.06

(FDD) builds objects layer-by-layer and thereby inducing variations in material properties and the presence of imperfections (such as voids and pores), depending on the different printing direction. These possible imperfections may influence the dissolution of PVA. Except for the printing direction (vertical/horizontal), thickness/radius and wax coating are also taken into consideration. Instead of solid tubes, hollow tubes were printed to minimize the outward expansion of the tubes caused by water uptake during the dissolution of PVA. Note that the printing quality of such hollow tubes tends to be poor if the tube thickness is small, since the diameter of heated nozzle used herein is 0.25 mm. On the other hand, thick tubes are difficult to dissolve due to the volume expansion. In addition, the volume expansion of the PVA tube wall may introduce cracks to the cementitious matrix, especially in the early age [30]. To determine the optimal thickness of the PVA tubes, PVA tubes with different thicknesses/radius (t/R) were fabricated and investigated.

It is known that PVA polymers react with $\text{Ca}(\text{OH})_2$ and Calcite (CaCO_3) in the cementitious matrix, and the reactant is not dissolvable [30]. In other words, the reaction has an adverse influence on the dissolution of PVA tubes. To isolate the PVA tubes from the cementitious matrix, the hollow PVA tubes were coated with wax. Wax coating was performed by spraying with paraffin wax with a low melting temperature. The dissolution of the coated PVA tubes and uncoated PVA tubes are compared. The samples embedded with PVA tubes were cured in water under room temperature for 7 days before being observed with X-ray computed tomography (CT scanning). The schematic of samples under different fabrication configuration is shown in Fig. 1. In the figure, t and R refer to the thickness and radius of the tubes, respectively.

After understanding the effect of printing direction, vascular tube thickness and coating condition, two-dimensional (2D) and three-dimensional (3D) vascular networks were fabricated. The diameters of the vascular network were designed based on Murray's law to minimise turbulent flow at junctions [39,40]. To avoid possible blockage caused by volume expansion during the dissolution of PVA tubes, the amount of PVA in the vascular network was minimized. In particular, the vascular network in the possible crack region (under 4-point bending load) was printed with PVA, with the remainder printed with PLA. The properties of PLA and PVA are shown in Table 2.

The 3D-printed vascular network is assembled and then embedded in the cementitious matrix. The schematics of the 3D-printed vascular

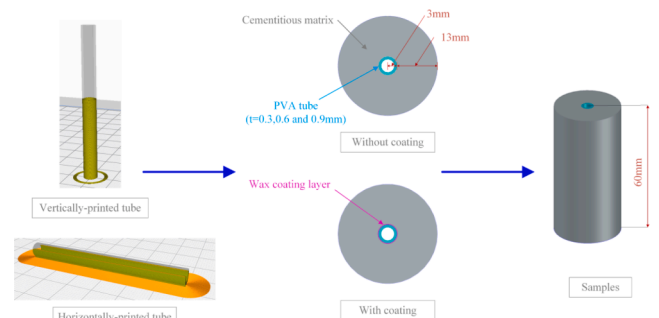


Fig. 1. Schematic of samples with PVA tubes under different configurations.

Table 2
The properties of PLA and PVA.

Property	PLA	PVA
Chemical formula	$(C_3H_4O_2)_x$	$(C_2H_4O)_x$
Glass transition ($^{\circ}C$)	~ 60	58.4
Melting temperature ($^{\circ}C$)	145–160	175.4
Specific gravity (g/cm 3)	1.24	1.23

networks in the cementitious matrix are shown in Fig. 2. For comparison, the parent tubes of the vascular network (PLA part) are kept in the middle of height in the samples for 2D and 3D vascular network (see Table 3).

2.2. Casting, removing vascular and curing

2.2.1. Casting

After the vascular networks were assembled and pre-processed (i.e., coated with wax), they were positioned in the foam moulds using pre-cast cement paste holders (see Fig. 2). Fibre reinforced mortar was used as the binder, with 0.1% of volume ultra-high molecular weight polyethylene fibre (UHMWPE) to prevent the samples from suddenly breaking into two halves during the 4-point bending test. The technical data sheet of UHMWPE and the mix proportion of the cementitious mortar are listed in Tables 3 and 4, respectively. Except the vascular based self-healing specimens, plain cementitious mortar (i.e., without vascular network) is tested as a reference. It is noted that there are 3 samples in each group, i.e., specimens with 2D vascular network, specimens with 3D vascular network and references (without vascular networks).

The casting process, similar to our earlier work [41], was as follows: cement and sand were dry-mixed for 4 min in a Hobart planetary mixer. Water was then added to the dry components and mixed for 2 min. Afterwards, fibres were added and mixed for another 2 min. The mixed materials were poured in Styrofoam moulds with a dimension of 160 mm \times 40 mm \times 40 mm and vibrated for 30 s. The specimens were covered with plastic film to prevent water loss. The specimens were kept in room temperature for 24 h and then demoulded.

2.2.2. Removing PVA vascular and curing

Considering that the dissolution of one-dimensional PVA tube is relatively easy, these samples were directly submerged in water with room temperature for 7 days to remove the PVA tube walls after demoulding. The curing water was daily changed considering a possible reaction between the dissolved PVA in water and cementitious matrix.

For the samples embedded with the 2D/3D PVA vascular network, more measures were taken to help remove the PVA tubes before the curing process. According to Li et al. [30], elevated temperature accelerates dissolution of PVA tubes. Therefore, demoulded samples were

submerged in hot water with a temperature of 70 $^{\circ}C$ in the first 2 h (from 24 to 26 h). At the same time, pressurized air was injected into the vascular networks to flush the dissolved PVA out of the network every 30 min (i.e., 4 times in 2 h) to avoid the blockage in the joints of the vascular networks. Afterwards, the samples were cured in water with room temperature for 27 days before the first round of the 4-point bending test. Curing water was changed every week.

2.3. Healing process

The samples were subjected to 4-point bending to measure the initial flexural strength as well as to induce cracks for the following healing process. Epoxy resin was used as the healing agent because of its low viscosity and high regain in strength [20]. Epoxy resin (Conpox Resin BY 158, Condor Kemi A/S) and hardener (Conpox Hardener BY 2996, Condor Kemi A/S) were first weighted and mixed with a mass ratio of 3:1 and stirred for 1 min. Then, epoxy resin was manually injected into the vascular networks from one end through a syringe while blocking the other end with a clip. In total, 10 ml of epoxy resin was used to ensure sufficient amount to reach the crack through the vascular. The injection speed was controlled as 10 ml/min. The clip was removed after 5 min, and then pressurized air was injected after 30 min to remove the excess epoxy resin from the hollow channels. The schematics of the manual healing process is shown in Fig. 3. The treated samples were kept at room temperature for 24 h until the injected epoxy resin was fully hardened. The healed samples were tested under 4-point bending (three samples in each group).

2.4. Characterization

2.4.1. Four-point bending test

To measure the initial flexural strength as well as the mechanical recovery of the cementitious mortar embedded with vascular networks, four-point bending tests were performed using a servo hydraulic press (INSTRON 8872). The specimens were loaded with a constant crack opening speed of 0.5 $\mu m/s$ with Linear Variable Differential Transformers (LVDTs), as recommended by Tziviloglou et al. [14]. The virgin specimens were loaded until the crack width reached 400 μm . The crack widths of the specimens after unloading were recorded as the final crack widths. After the healing process, the specimens were loaded again until the crack width reached 400 μm again. The setup of 4-point bending test with two horizontal Linear Variable Differential Transformers (LVDTs) is shown in Fig. 4. It is worth mentioning that the LVDT (length = 50 mm) was positioned in the region with PVA tubes (length = 60 mm) in the middle span of the prismatic samples. The healing process was carried out multiple healing cycles, until it is difficult to manually inject the epoxy resin into the crack. For each 4-point bending test, the specimens were loaded until the crack width reached 400 μm . The flexural strength in each test was recorded and compared.

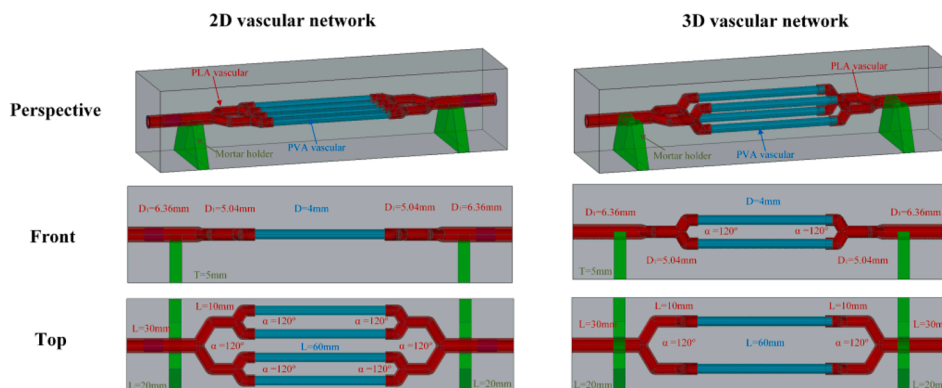


Fig. 2. Schematic of samples embedded with 3D-printed PVA vascular network.

Table 3
The technical data sheet of ultra-high molecular weight polyethylene fibre (UHMWPE).

Density (g/cm ³)	Length (mm)	Filament cross section	Filament diameter (μm)	Melting range (°C)	Breaking Strength (GPa)	Breaking Modulus (GPa)	Elongation (%)
0.97–0.98	6	Nearly round	19–43	144–152	3.0	110	2–3

Table 4
Mix design of the cementitious matrix (kg/m³).

CEM III/B	Sand	water	UHMWPE
42.5N	(0.125–0.25 mm)		
1200	550	480	1

2.4.2. Permeability test

To evaluate the water tightness before and after the healing process, the test method proposed by Tziviloglou et al. [14] was used in this study. During the test, one end of the vascular network was blocked with a clip while the other end was connected to a tube. The other end of vascular network was connected to a water container with a water head of 0.75 m from the upper surface of the tested specimens. The amount of leaked water before and after the 4-point bending tests was recorded and compared. The schematics of the experimental setup for watertightness evaluation is shown in Fig. 5.

2.4.3. CT scanning

The dissolutions of 3D-printed PVA tubes as well as the PVA vascular network embedded in the cementitious mortar were observed using a micro-CT scanner (Phoenix Nanotom). The microstructures were reconstructed using the dedicated Phoenix Dotos software. The resolution of the obtained slice for hollow tubes is 5 μm. For the self-healing cementitious composite embedded with PVA vascular network, the middle span of hardened samples (PVA part of the vascular networks) was scanned to observe the inner structure of vascular network with a resolution of 27.5 μm.

3. Results and discussion

3.1. Influence of printing configuration on dissolution of PVA

3.1.1. Dissolution of one-dimensional PVA tubes

According to previous studies [19,42], properties of the 3D-printed structures are significantly influenced by the printing parameters such as printing direction and printing layer-height. Herein, the influence of printing direction on the dissolution of PVA vascular is first studied using one-dimensional hollow bars. Besides, thickness and wax coating are also considered. Directly observing from the surface of the

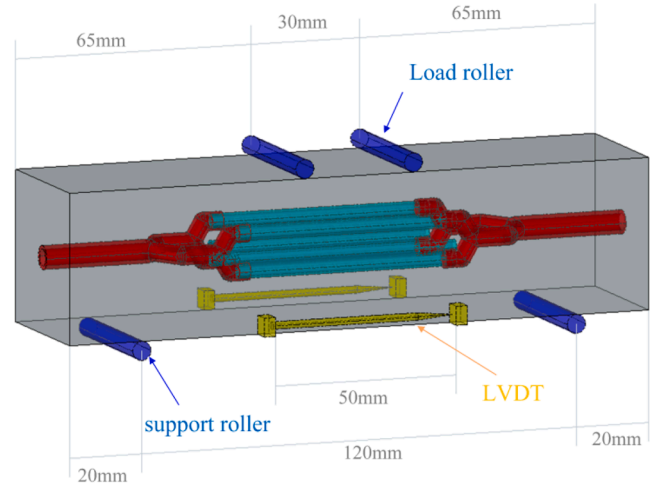


Fig. 4. Schematic of four-point bending test.

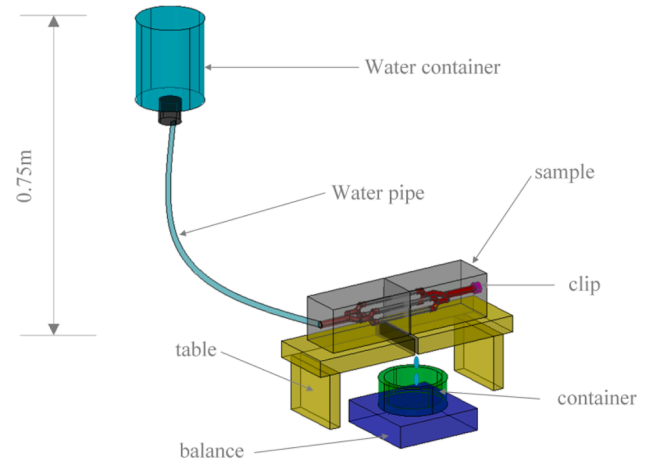


Fig. 5. Schematics of permeability test setup.

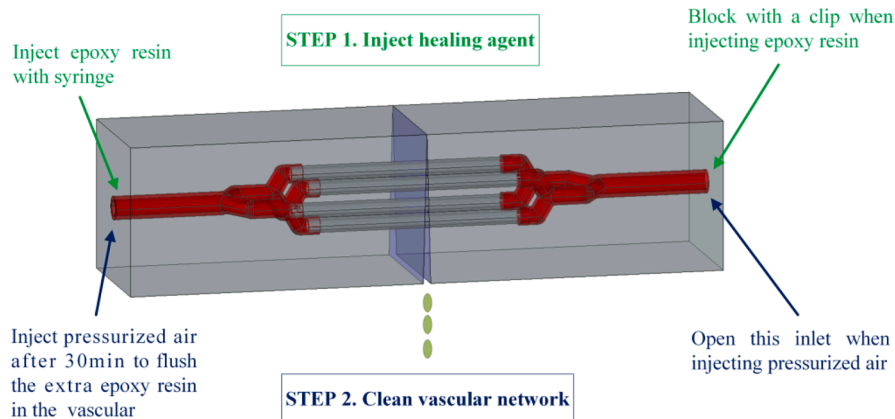


Fig. 3. Schematic of manual healing process (3D vascular network).

demoulded samples and the result is shown in Table 5.

From the table, it noted that the horizontally printed tubes without wax coating did not dissolve. Therefore, the inner parts of those samples were not investigated with micro-CT scanner. The tomographs of tested samples are shown in Fig. 6. The black part in the figures represents the air, manifesting that nothing exists there.

As shown in Fig. 6(a), the dissolution of PVA tubes is significantly influenced by printing direction and coating condition. When the thickness/radius is 0.2 and the tubes are wax coated, the vertically printed tube dissolved better than the horizontally printed one. For the horizontally printed PVA tube, the tube wall has not fully dissolved, and several cracks are present in the cementitious matrix around the tubes. A possible reason is the poor printing quality of the horizontally printed tube, resulting in more defects. Consequently, a part of the PVA tube is not insulated from the cementitious matrix even though the PVA tube was coated with paraffin wax. The rough interface between PVA tube and matrix (0.2-horizontal-wax coating) shows that the PVA tube reacts with the cementitious matrix, causing it to expand. As a result, cracks occur in the matrix around the tubes. In vertically printed tubes (0.2-vertical-wax coating), PVA dissolved almost completely and no cracks occur around the tube. The interface between the cementitious matrix and the tube is smoother compared to that of the horizontally printed one. Therefore, printing the PVA tube in a vertical direction to compose the vascular networks.

Except for printing direction, wax coating also significantly influences the dissolution of PVA tubes (Fig. 6(a)). Compared with the coated PVA tubes (0.2-vertical-coating), the uncoated tube (0.2-vertical-No coating) did not dissolve at all. The reaction between the cementitious matrix and PVA causes problems for both cementitious matrix and PVA tube. On one hand, the reacted mortar around the tubes delaminates with other matrix and thereby causing cracks in the matrix, while the reacted PVA fails to dissolve. On the other hand, the inner PVA wall expands inwards and fills the inner space due to the water uptake. This makes it impossible for water to enter the tube which then ceases to dissolve.

The influence of tube wall thickness/radius ratio (0.1–0.3) is also investigated. As shown in Fig. 6(b), the dissolution of PVA tube with thickness/radius ratio of 0.1 is the poorest, although a part of the tube has been removed. Compared with the thicker tube, less perimeter lines are used for the thin wall (thickness = 0.2 mm, $t/R = 0.1$) and thereby causing unstable printing, which increases the possibility of more defects. As a result, wax coating was not uniform and the reaction between PVA and cementitious mortar occurred locally in the areas of defects. For thickness/radius ratios of 0.2 and 0.3, the PVA tubes are totally dissolved. Considering that the thick PVA tube not only consumes more printing material, but also takes more time to dissolve, the thickness/radius ratio of 0.2 was selected for further investigation in this study.

Therefore, the PVA parts of the vascular networks were printed in the vertical direction, which showed better printing quality compared with the horizontally printed counterparts. Furthermore, wax coating proved to be necessary for the dissolution of PVA tubes by isolating the PVA tubes from the cementitious matrix and thereby preventing the occurrence of their expansive reaction. Based on the thickness/radius ratio, the thickness of PVA tube is set as 0.4 mm (radius is 2 mm) for creating the middle part of the vascular networks. The outer part of the vascular network is created with PLA. To decrease the scaffold during the printing process, the PLA parts of the 2D/3D vascular networks are printed in horizontal and vertical respectively. Those two parts (i.e., PVA tubes and PLA connectors) were assembled and sealed with liquid rubber (Bison rubber repair) to avoid leakage. Wax coating for the PVA tubes was applied after assembling. The 3D-printed vascular networks are shown in Fig. 7. The actual thickness of the 3D-printed PVA tubes is measured by microscope (Keyence VHX Digital Microscope). From the result, it could be concluded that there are inaccuracies during the printing process.

3.1.2. Dissolution of the 3D-printed vascular network

Based on the result in 3.1.1, vascular networks were created and embedded in the cementitious mortar. To observe the dissolution of the PVA part of the network, CT scanning was performed out before the mechanical tests. The results are shown in Fig. 8.

From Fig. 8, it is obvious that majority of the PVA tubes in the 2D and 3D vascular network have dissolved. Furthermore, there were no issues in connecting the PLA and PVA tubes using liquid rubber, which was confirmed because the cementitious slurry did not enter the vascular network through these connection points. However, compared with the one-dimensional tubes studied Section 3.1.1, the overall dissolution of PVA is less efficient. The PVA tubes are in the middle part of the vascular network, making it difficult for the dissolved PVA to flow out of the vascular networks. As a result, some PVA remained in hollow vascular network for both geometries (i.e., 2D and 3D).

The PVA tubes in the 2D vascular network had poorer dissolution compared with those in the 3D vascular network. As shown in the Fig. 8 (a), part of the PVA tubes fails to dissolve in the middle part of 2D vascular network, while no PVA remained in the middle of the 3D vascular network. Furthermore, cracks connecting the hollow channels occurred in the 2D vascular network, while the cracks are less obvious in 3D vascular network. As a result, the dissolution of the PVA tubes in the 3D vascular network outperforms that of the 2D vascular network.

Although the PVA tube wall in the vascular network is well removed, some problems did occur during casting and pre-processing. Compared with the designed vascular network orientation, the position of the vascular networks is slightly changed for both 2D and 3D vascular network and it may bring some problems when the accurate orientation of vascular network is required. Besides, some cracks occur around the channels for both 2D and 3D vascular network. These could have been caused to an extent by the pressurized air used to remove the dissolved PVA. It is noteworthy that the wax/PVA dissolvable network system is scalable. For large-scale structural elements, the fabrication of the network system (larger diameters) and wax coating (larger thickness) are relatively easy. Besides, previous similar researches show the feasibility of injecting hot water in large vascular network [43]. However, the pressure has to be increased for large-scale structures.

3.2. Flexural strength

3.2.1. Initial flexural response of the vascular based self-healing composite

The existence of vascular network has great influences on the initial flexural strength of vascular based self-healing cementitious composites. For all the specimens, cracks occur in the middle span between the two load rollers. In other words, cracks do not hit the PLA connectors of the vascular network. The stress-crack width (CMOD) curves of the cementitious mortar embedded with 2D and 3D vascular network are shown in Fig. 9.

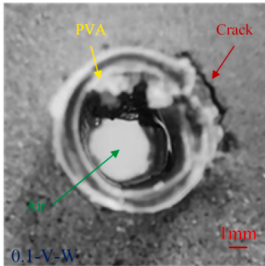
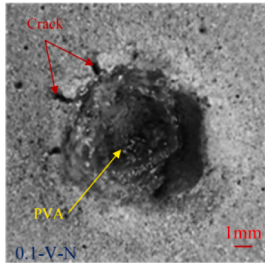
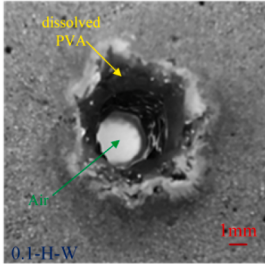
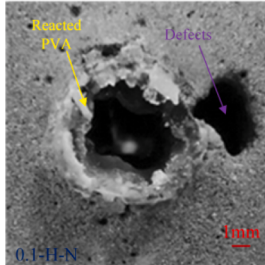
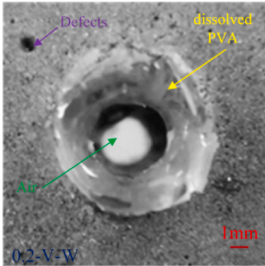
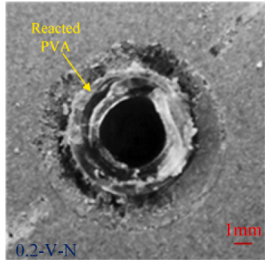
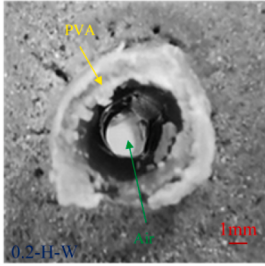
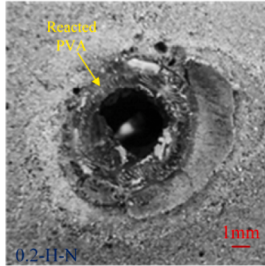
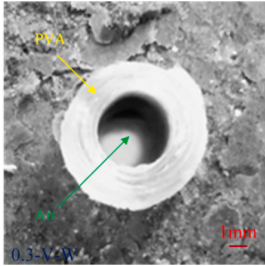
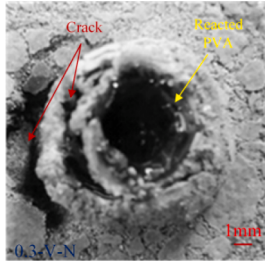
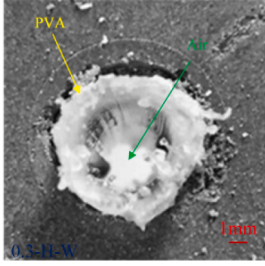
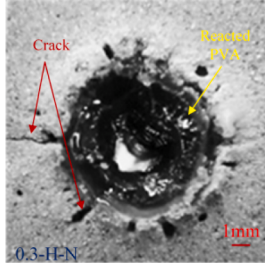
From Fig. 9, it is found that the flexural strength of the specimens with hollow vascular networks is lower than the references, showing that the existence of vascular network has adverse effects on the flexural strength. This is in agreement with previous studies [27]. Note that, although the small amount fibres (0.1% by volume) give the specimens some residual load-bearing capacity, only one crack is observed in all samples. Compared with the references, the vascular based self-healing mortar have lower residual load-bearing capacity.

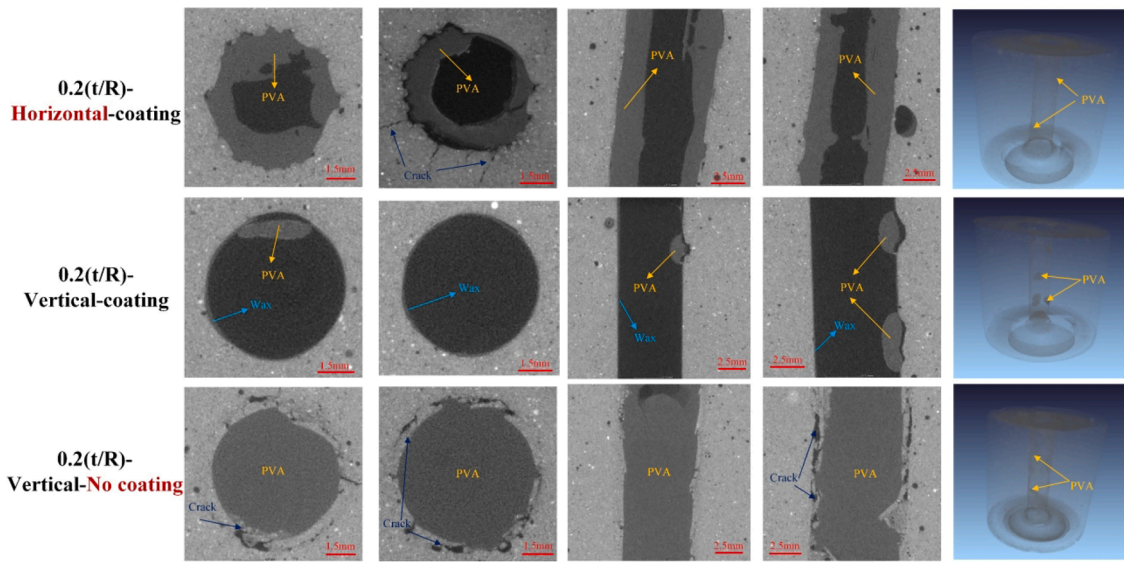
As to the influence of vascular network shape, there is no significant difference between samples with 2D and 3D hollow vascular networks: the mean flexural strength of 2D vascular based self-healing cementitious mortar is slightly higher, but with less standard deviation compared to the 3D counterpart. For both 2D and 3D vascular based self-healing specimens, crack closure occurs and the final crack widths of samples are less than 400 μm .

3.2.2. Mechanical recovery of the vascular based self-healing composite

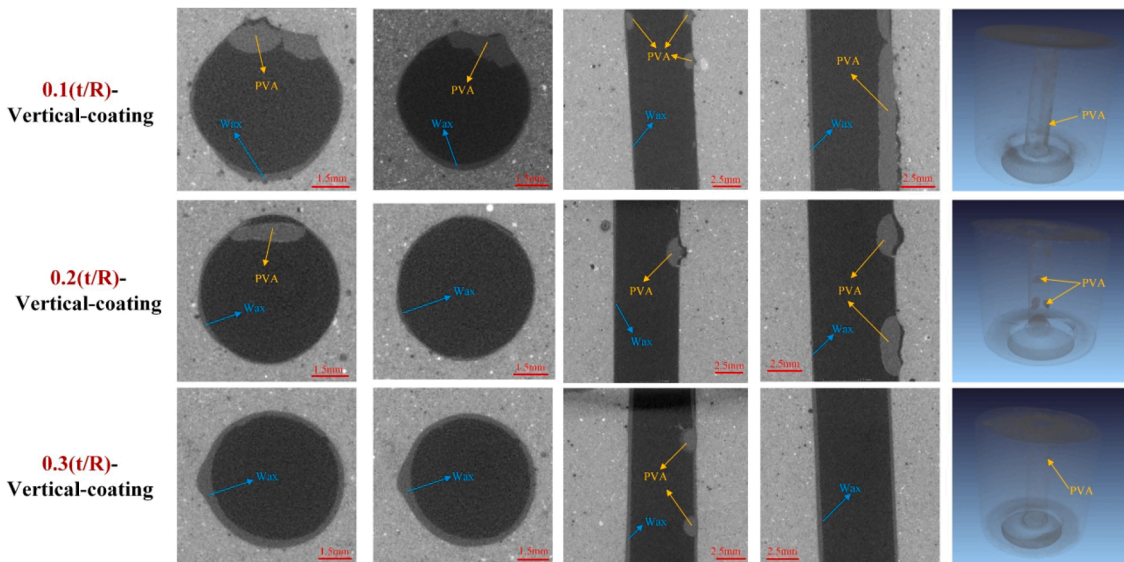
To seal the cracks, epoxy resin was injected through the vascular

Table 5
Dissolution of PVA for the demoulded samples.

Printing configurations (r/R-printing direction)	Wax coating	No wax coating
0.1-Vertical		
0.1- Horizontal		
0.2-Vertical		
0.2- Horizontal		
0.3-Vertical		
0.3- Horizontal		



(a) Tubes with different printing direction and wax coating



(b) Tube with different thickness/radius

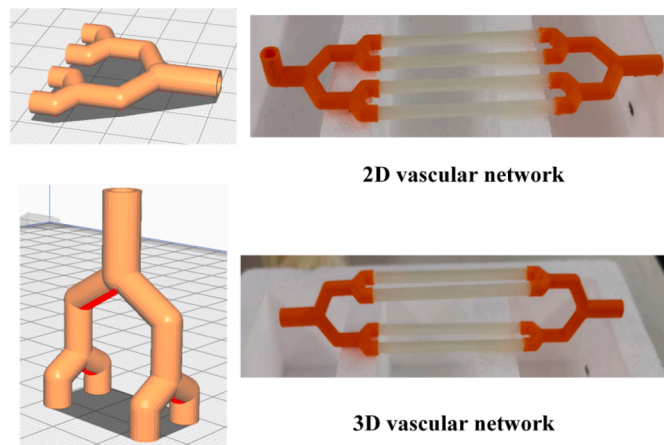
Fig. 6. Test result from CT scanning, (a) Tubes with different printing direction and wax coating (thickness/radius of 0.2); (b) Tube with different thickness/radius (vertically printed, wax coating).

networks. The healed samples were tested again after the epoxy resin had hardened. Multiple healing processes were carried out until it became difficult to manually inject the epoxy resin to the vascular networks. Based on the test, we performed two healing cycles for 2D vascular based self-healing concrete, while performing three cycles for the samples embedded with the 3D vascular network. The flexural responses of samples embedded with 2D/3D vascular networks are shown in Fig. 10.

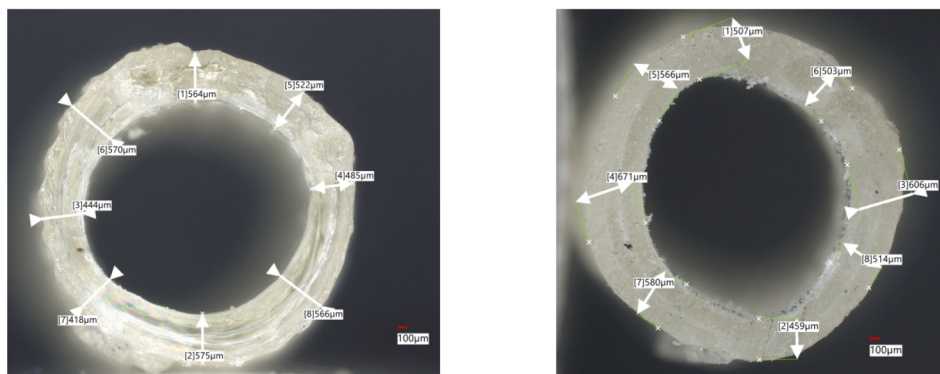
As shown in Fig. 10, flexural strength can be regained upon healing in vascular based self-healing cementitious mortar. Compared with reference specimens, the specimens with vascular networks have higher flexural strength after the first healing process, manifested with healing efficiencies higher than 100%. In addition, the specimens after healing, the residual load-bearing capacity of the specimens increased. This may be caused by the fact that the interface between fibres and cementitious

matrix in the crack also are also reinforced by the injected epoxy resin. According to the previous research [44], fibre/matrix interface can be enhanced due to the increase of the interfacial frictional bond strength of FRCC after autogenous healing.

After the second healing process, the flexural strength is still higher than the initial one. However, the flexural strength after the second healing process is lower than that after the first healing. This was observed for both 2D and 3D vascular based self-healing composite mortar. A possible reason is that the epoxy resin injected in the first healing process hardened in the vascular, although pressurized air was used to remove the excess epoxy resin from the vascular network. As a result, less epoxy resin flows into the crack during the second healing process. Compared with the 2D vascular specimens, the flexural strength of the 3D vascular specimens after the second healing cycle is higher. Besides, the samples embedded with 3D vascular network were healed



(a) Schematic of vascular network



(b) Actual thickness of the 3D-printed PVA tube

Fig. 7. Fabrication of vascular network (a) schematic of the 2D-/3D- vascular network (orange- PLA, white- PVA); (b) Actual thickness of 3D-printed PVA tube. (For interpretation of the references to colour in this figure legend, the reader is referred to the web version of this article.)

for 3 rounds. Therefore, the samples embedded with 3D vascular network have higher healing potential. In terms of residual load-bearing capacity after cracking, 2D vascular based specimens perform better than 3D vascular specimens after the second healing cycle.

3.3. Water tightness

3.3.1. Water tightness recovery

Except from strength regain, water tightness is also of great importance. Permeability tests were carried out on cracked specimens before and after the self-healing procedure. The water tightness was measured after each 4-point bending test and healing process. The recovery of water tightness is defined in as [14]:

$$RWT = \frac{W_{n-h}(t) - W_h(t)}{W_{n-h}(t)} \times 100\% \quad (1)$$

where $W_{n-h}(t)$ and $W_h(t)$ are the average amount of water that has passed through the unhealed and healed cracks of the specimens per second (unit in g/s), respectively.

The amounts of leaked water through the healed cracks of the 2D/3D vascular based self-healing cementitious specimens are 0 after each healing process. Therefore, the water tightness of the investigated specimens has fully recovered (i.e., $RWT = 100\%$). One possible reason for the high recovery of water tightness is that the fibres in the cracks

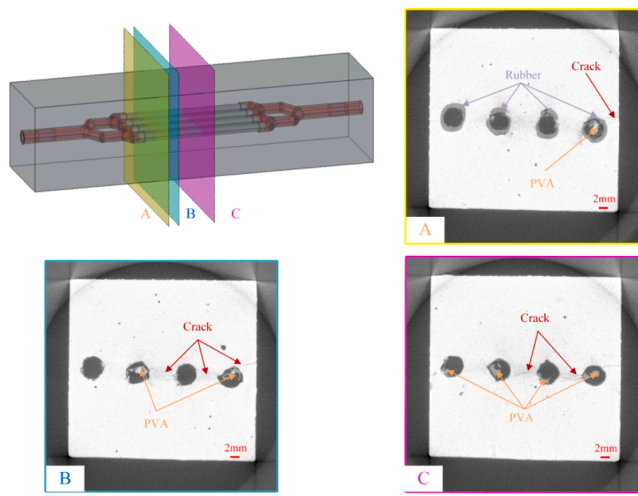
increase the roughness of crack, promoting the injected epoxy resin to remain in the cracks instead of flowing out the cracks. It should be noted, however, the permeability test setup used only with a water head of 0.75 m, which made it difficult to measure low values of flow speed.

3.3.2. Crack water tightness after healing process

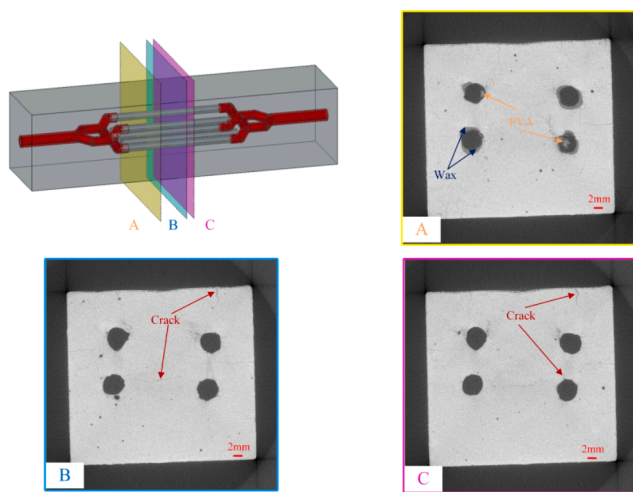
Except for water tightness recovery, the water tightness of the cracked samples was also investigated since several healing processes were carried out. The watertightness of the cracked specimens could help judge whether it is possible to carry out the next round of healing process. The mean watertightness of the specimens embedded with 2D/3D vascular network are shown in Fig. 11.

From Fig. 11, the mean watertightness of the original samples embedded with 3D vascular network is much larger than that of the 2D vascular ones. A possible reason is that two channels of the 3D vascular network are closer to the bottom. With the increased number of healing cycles, the watertightness of the cracked samples decreases for both 2D and 3D vascular based self-healing cementitious mortar. This is caused by hardening of increasing residual epoxy resin in the vascular network.

Compared with the samples with 3D vascular networks, the watertightness of the 2D vascular based self-healing concrete is lower after each 4-point bending test. However, this may decrease the possibility of further healing, because the low watertightness will also prevent the healing agent (i.e., epoxy resin) from entering the crack. This could also

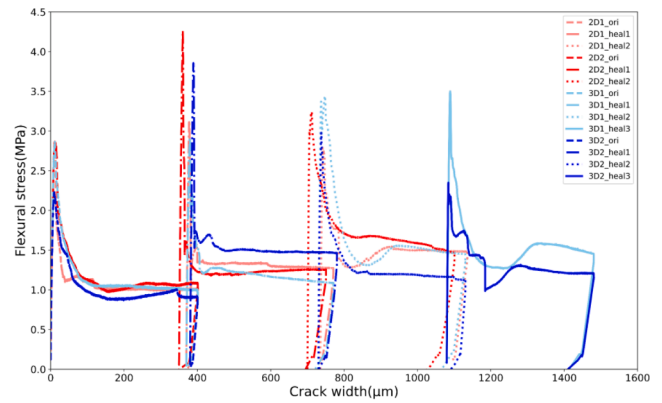


(a) PVA tubes in a 2D vascular network

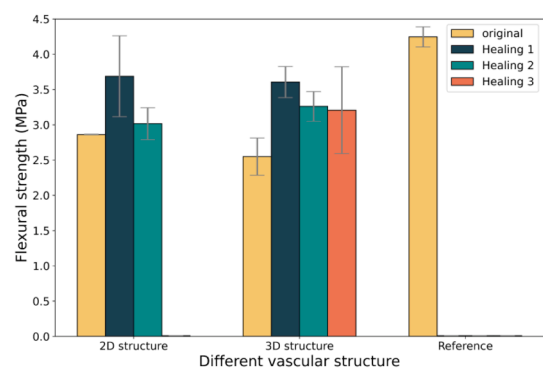


(b) PVA tubes in a 3D vascular network

Fig. 8. CT scans of vascular based self-healing concrete. (a) PVA tube in the 2D vascular network; (b) PVA tube in the 3D vascular network.



(a) Flexural response comparison of the healed samples



(b) Flexural strength comparison of the healed samples

Fig. 10. Comparison of the healed specimens embedded with 2D-/3D- vascular network regarding (a) flexural response; (b) flexural strength.

be explained why the flexural strength of 3D vascular based self-healing concrete is higher than that of the 2D vascular samples after the second healing process. As a result, 3D vascular network enables performing more healing processes than the 2D vascular network for the vascular based self-healing concretes.

4. Conclusions

Herein, a self-healing concrete was developed using 3D printed sacrificial vascular networks. Thereby, the influence of vascular printing direction, thickness/radius and wax coating on the dissolution of one-dimensional PVA tubes was first investigated. Under the optimal printing configuration, two kinds of vascular networks (i.e., 2D/3D) with PVA tubes in the middle span were fabricated and embedded in the cementitious mortar. Four-point bending tests were carried out to evaluate the flexural strength as well as the mechanical recovery after healing. Furthermore, crack water tightness test of the 2D and 3D vascular based self-healing cementitious mortar was performed to investigate the watertightness of samples before and after healing. Based on the obtained results, the following conclusions can be drawn:

- (1) The reaction between PVA and cementitious matrix prevents the PVA tubes from dissolving, making coating on the tubes necessary (e.g., with wax, as done herein). The dissolution of vertically printed PVA tubes is better than of the horizontally printed ones. The less perimeter lines of thick tube results in unstable printing,

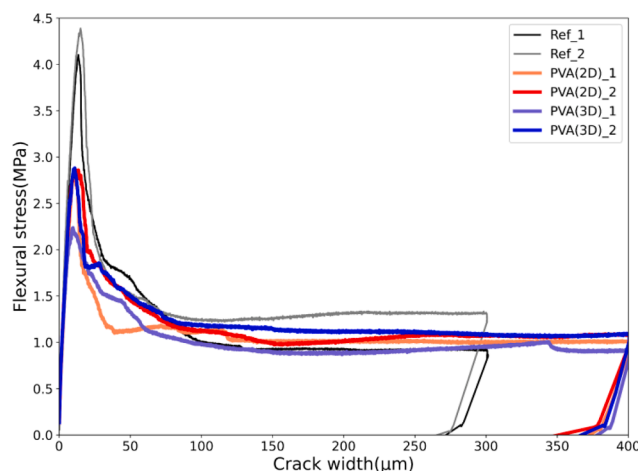
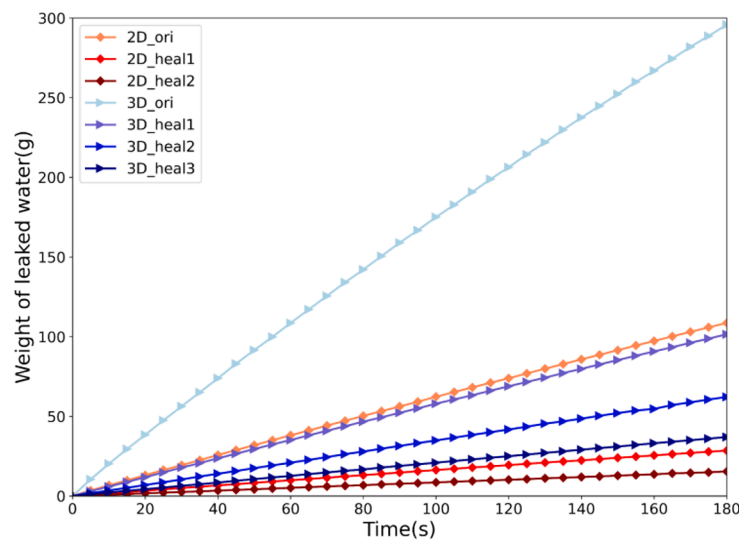
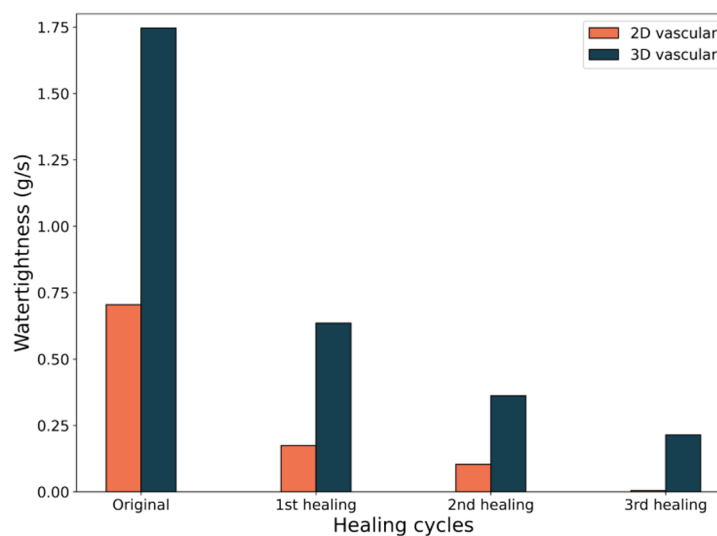


Fig. 9. Flexural response of specimens embedded with 2D/3D vascular networks.



(a) The change of leaked water with time



(b) Comparison of watertightness in different healing cycles

Fig. 11. Watertightness of the cracked specimens after 4-point bending tests; (a) The change of leaked water with time; (b) Water tightness comparison in different healing cycles.

which also affects the dissolution of PVA. The dissolution of PVA part in the 2D/3D vascular networks is excellent, as shown by X-ray tomography.

- (2) The existence of vascular network has adverse influences on the initial flexural strength. The mechanical recovery after each healing process is over 100% compared with the original specimens. The flexural strength after the first healing process is higher than after the second healing process. This is inferred to be caused by the extra hardened epoxy resin in the vascular network.
- (3) Except for the improvement of flexural strength, the residual flexural stress of the healed samples is higher than the original specimens. One possible reason is that the interface between fibres in the crack and cementitious matrix is strengthened by the injected epoxy resin.

- (4) The watertightness of the cracked 3D vascular specimens is much larger than of the 2D counterpart after the first 4-point bending test. However, the water tightness recovery of the 2D and 3D vascular based self-healing concretes are both 100% when performing crack water tightness test with a water head of 0.75 m. Besides, the water tightness of the cracked samples sees an increase as the healing process increases. However, the low watertightness will bring some problems for the following healing process. Therefore, the cementitious mortar embedded with 3D vascular network has higher healing potential than the one with 2D vascular network.

CRediT authorship contribution statement

Zhi Wan: Conceptualization, Methodology, Data curation, Writing –

original draft, Software. **Yu Zhang**: Data curation, Writing – review & editing. **Yading Xu**: Conceptualization, Writing – reviewing & editing. **Branko Šavija**: Supervision, Conceptualization, Methodology, Writing – reviewing & editing.

Declaration of Competing Interest

The authors declare that they have no known competing financial interests or personal relationships that could have appeared to influence the work reported in this paper.

Data availability

Data will be made available on request.

Acknowledgement

Zhi Wan and Yu Zhang would like to acknowledge the financial support of the China Scholarship Council (CSC) under the grant agreement No.201906220205 and No. 201808320456. Yading Xu and Branko Šavija acknowledge the financial support of the European Research Council (ERC) within the framework of the ERC Starting Grant Project “Auxetic Cementitious Composites by 3D printing (ACC-3D)”, Grant Agreement Number 101041342. The authors would like to acknowledge Mr. Maiko van Leeuwen and Mr. Arjan Thijssen for their support in mechanical tests and CT scanning tests.

References

- De Belie N, Gruyaert E, Al-Tabbaa A, Antonaci P, Baera C, Bajare D, et al. A Review of Self-Healing Concrete for Damage Management of Structures. *Adv Mater Interfaces* 2018;5:1800074. <https://doi.org/10.1002/ADML.201800074>.
- Hilloulin B, Hilloulin D, Grondin F, Loukili A, De Belie N. Mechanical regains due to self-healing in cementitious materials: Experimental measurements and micro-mechanical model. *Cem Concr Res* 2016;80:21–32. <https://doi.org/10.1016/j.cemconres.2015.11.005>.
- Van Tittelboom K, De Belie N. Self-healing in cementitious materials—a review. *Materials (Basel)* 2013;6:2182–217. <https://doi.org/10.3390/ma6062182>.
- Sahmaran M, Yildirim G, Erdem TK. Self-healing capability of cementitious composites incorporating different supplementary cementitious materials. *Cem Concr Compos* 2013;35:89–101. <https://doi.org/10.1016/j.cemconcomp.2012.08.013>.
- Termkhajornkit P, Nawa T, Yamashiro Y, Saito T. Self-healing ability of fly ash-cement systems. *Cem Concr Compos* 2009;31:195–203. <https://doi.org/10.1016/j.cemconcomp.2008.12.009>.
- Ferrara L, Krelani V, Carsana M. A “fracture testing” based approach to assess crack healing of concrete with and without crystalline admixtures. *Constr Build Mater* 2014;68:535–51. <https://doi.org/10.1016/j.conbuildmat.2014.07.008>.
- Ferrara L, Krelani V, Moretti F. On the use of crystalline admixtures in cement based construction materials: from porosity reducers to promoters of self healing. *Smart Mater Struct* 2016;25:084002. <https://doi.org/10.1088/0964-1726/25/8/084002>.
- Rodríguez CR, Figueiredo SC, Deprez M, Snoeck D, Schlangen E, Šavija B. Numerical investigation of crack self-sealing in cement-based composites with superabsorbent polymers. *Cem Concr Compos* 2019;104:103395. <https://doi.org/10.1016/j.cemconcomp.2019.103395>.
- Gruyaert E, Debbaut B, Snoeck D, Díaz P, Arizo A, Tziviloglou E, et al. Self-healing mortar with pH-sensitive superabsorbent polymers: testing of the sealing efficiency by water flow tests. *Smart Mater Struct* 2016;25:084007. <https://doi.org/10.1088/0964-1726/25/8/084007>.
- B. Corina-Maria Aldea, W.-J. Song, J.S. Popovics, A. Member, S.P. Shah, Extent of Healing of Cracked Normal Strength Concrete, *J. Mater. Civ. Eng.* 12 (2000) 92–96. [https://doi.org/10.1061/\(ASCE\)0899-1561\(2000\)12:1\(92\)](https://doi.org/10.1061/(ASCE)0899-1561(2000)12:1(92)).
- Šavija B, Feiteira J, Araújo M, Chatrabhuti S, Raquez JM, Van Tittelboom K, et al. Simulation-aided design of tubular polymeric capsules for self-healing concrete. *Materials (Basel)* 2017;10:10. <https://doi.org/10.3390/ma10010010>.
- Lv LY, Zhang H, Schlangen E, Yang Z, Xing F. Experimental and numerical study of crack behaviour for capsule-based self-healing cementitious materials. *Constr Build Mater* 2017;156:219–29. <https://doi.org/10.1016/j.conbuildmat.2017.08.157>.
- Kanellopoulos A, Giannaros P, Palmer D, Kerr A, Al-Tabbaa A. Polymeric microcapsules with switchable mechanical properties for self-healing concrete: Synthesis, characterisation and proof of concept. *Smart Mater Struct* 2017;26:045025. <https://doi.org/10.1088/1361-665X/aa516c>.
- Tziviloglou E, Wiktor V, Jonkers HM, Schlangen E. Bacteria-based self-healing concrete to increase liquid tightness of cracks. *Constr Build Mater* 2016;122: 118–25. <https://doi.org/10.1016/j.conbuildmat.2016.06.080>.
- González Á, Parraguez A, Corvalán L, Correa N, Castro J, Stuckrath C, et al. Evaluation of Portland and Pozzolanic cement on the self-healing of mortars with calcium lactate and bacteria. *Constr Build Mater* 2020;257:119558. <https://doi.org/10.1016/j.conbuildmat.2020.119558>.
- Tziviloglou E, Pan Z, Jonkers HM, Schlangen E. Bio-based self-healing mortar: An experimental and numerical study. *J Adv Concr Technol* 2017;15:536–43. <https://doi.org/10.3151/jact.15.536>.
- Lee MW, An S, Yoon SS, Yarin AL. Advances in self-healing materials based on vascular networks with mechanical self-repair characteristics. *Adv Colloid Interface Sci* 2018;252:21–37. <https://doi.org/10.1016/j.cis.2017.12.010>.
- Hamilton AR, Sottos NR, White SR. Self-healing of internal damage in synthetic vascular materials. *Adv Mater* 2010;22:5159–63. <https://doi.org/10.1002/adma.201002561>.
- Wan Z, Xu Y, Zhang Y, He S, Šavija B. Mechanical properties and healing efficiency of 3D-printed ABS vascular based self-healing cementitious composite: Experiments and modelling. *Eng Fract Mech* 2022;267:108471. <https://doi.org/10.1016/j.engfracmech.2022.108471>.
- Shields Y, Van Mullem T, De Belie N, Van Tittelboom K. An Investigation of Suitable Healing Agents for Vascular-Based Self-Healing in Cementitious Materials. *Sustain.* 2021, Vol. 13, Page 12948. 13 (2021) 12948. <https://doi.org/10.3390/SU132312948>.
- Snoeck D, De Belie N. Repeated Autogenous Healing in Strain-Hardening Cementitious Composites by Using Superabsorbent Polymers. *J Mater Civ Eng* 2016;28:1–11. [https://doi.org/10.1061/\(asce\)mt.1943-5533.0001360](https://doi.org/10.1061/(asce)mt.1943-5533.0001360).
- Yerro O, Radojevic V, Radovic I, Petrovic M, Uskokovic PS, Stojanovic DB, et al. Thermoplastic acrylic resin with self-healing properties. *Polym Eng Sci* 2016;56: 251–7. <https://doi.org/10.1002/pen.24244>.
- Dry CM. Three designs for the internal release of sealants, adhesives, and waterproofing chemicals into concrete to reduce permeability. *Cem Concr Res* 2000;30:1969–77. [https://doi.org/10.1016/S0008-8846\(00\)00415-4](https://doi.org/10.1016/S0008-8846(00)00415-4).
- Li VC, Lim YM, Chan YW. Feasibility study of a passive smart self-healing cementitious composite. *Compos Part B Eng* 1998;29:819–27. [https://doi.org/10.1016/S1359-8368\(98\)00034-1](https://doi.org/10.1016/S1359-8368(98)00034-1).
- Minnebo P, Thierens G, De Valck G, Van Tittelboom K, De Belie N, Van Hemelrijck D, et al. A novel design of autonomously healed concrete: Towards a vascular healing network. *Materials (Basel)* 2017;10:49. <https://doi.org/10.3390/ma10010049>.
- Williams HR, Trask RS, Bond IP. Self-healing composite sandwich structures. *Smart Mater Struct* 2007;16:1198–207. <https://doi.org/10.1088/0964-1726/16/4/031>.
- Li Z, de Souza LR, Litina C, Markaki AE, Al-Tabbaa A. A novel biomimetic design of a 3D vascular structure for self-healing in cementitious materials using Murray’s law. *Mater Des* 2020;190:108572. <https://doi.org/10.1016/j.matdes.2020.108572>.
- Xu Y, Zhang H, Gan Y, Šavija B. Cementitious composites reinforced with 3D printed functionally graded polymeric lattice structures: Experiments and modelling. *Addit Manuf* 2021;39:101887. <https://doi.org/10.1016/j.addma.2021.101887>.
- Xu Y, Šavija B. Development of strain hardening cementitious composite (SHCC) reinforced with 3D printed polymeric reinforcement: Mechanical properties. *Compos Part B Eng* 2019;174. <https://doi.org/10.1016/j.compositesb.2019.107011>.
- Li Z, de Souza LR, Litina C, Markaki AE, Al-Tabbaa A. Feasibility of Using 3D Printed Polyvinyl Alcohol (PVA) for Creating Self-Healing Vascular Tunnels in Cement System. *Materials (Basel)* 2019;12:3872. <https://doi.org/10.3390/ma12233872>.
- Toohy KS, Sottos NR, Lewis JA, Moore JS, White SR. Self-healing materials with microvascular networks. *Nat Mater* 2007;6:581–5. <https://doi.org/10.1038/nmat1934>.
- Patrick JF, Hart KR, Krull BP, Diesendruck CE, Moore JS, White SR, et al. Continuous self-healing life cycle in vascularized structural composites. *Adv Mater* 2014;26:4302–8. <https://doi.org/10.1002/adma.201400248>.
- Boba K, Heath C, Bond IP, Wass DF. Novel Manufacturing Method for FRP Composites With a Multifunctional Vascular Network, 4th Int. Conf Self-Healing Mater 2013:388–91.
- Pareek S, Oohira A. A fundamental study on regain of flexural strength of mortars by using a self-repair network system. In: *Proc. 3rd Int. Conf. Self Heal. Mater., Bath, UK, 2011*: p. Vol. 2729.
- Sangadji S, Schlangen E. Self healing of concrete structures - Novel approach using porous network concrete. *J Adv Concr Technol* 2012;10:185–94. <https://doi.org/10.3151/jact.10.185>.
- Davies RE, Jefferson A, Lark R, Gardner D. A novel 2D vascular network in cementitious materials, (2015).
- Wan Z, Chang Z, Xu Y, Šavija B. Optimization of vascular structure of self-healing concrete using deep neural network (DNN). *Constr Build Mater* 2023;364:129955. <https://doi.org/10.1016/j.conbuildmat.2022.129955>.
- Dwiyati ST, Kholil A, Riyadi R, Putra SE. Influence of layer thickness and 3D printing direction on tensile properties of ABS material. *J Phys Conf Ser* 2019; 1402:2–8. <https://doi.org/10.1088/1742-6596/1402/6/066014>.
- Murray CD. The physiological principle of minimum work applied to the angle of branching of arteries. *J Gen Physiol* 1926;9:835–41. <https://doi.org/10.1085/jgp.9.6.835>.
- Murray CD. The Physiological Principle of Minimum Work. *Proc Natl Acad Sci* 1926;12:207–14. <https://doi.org/10.1073/pnas.12.3.207>.
- Xu Y, Schlangen E, Luković M, Šavija B. Tunable mechanical behavior of auxetic cementitious cellular composites (CCCs): Experiments and simulations. *Constr*

- Build Mater 2021;266:121388. <https://doi.org/10.1016/j.conbuildmat.2020.121388>.
- [42] Xu Y, Zhang H, Šavija B, Chaves Figueiredo S, Schlangen E. Deformation and fracture of 3D printed disordered lattice materials: Experiments and modeling. Mater Des 2019;162:143–53. <https://doi.org/10.1016/j.matdes.2018.11.047>.
- [43] Davies R, Jefferson T, Gardner D. Development and Testing of Vascular Networks for Self-Healing Cementitious Materials, (2021). [https://doi.org/10.1061/\(ASCE\)MT.1943-5533.0003802](https://doi.org/10.1061/(ASCE)MT.1943-5533.0003802).
- [44] Qiu J, He S, Yang EH. Autogenous healing and its enhancement of interface between micro polymeric fiber and hydraulic cement matrix. Cem Concr Res 2019; 124:105830. <https://doi.org/10.1016/j.cemconres.2019.105830>.